International Journal of Chemical Science
Online ISSN: 2523-2843, Print ISSN: 2523-6075; Impact Factor: RJIF 5.22
Received: 26-05-2019; Accepted: 28-06-2019
www.chemicaljournals.com
Volume 3; Issue 4; July 2019; Page No. 101-108

Nanomaterial and its spectral, electrical and magnetic properties

Saema Salim
Department of Chemistry, University of Management and Technology Lahore, Pakistan

Abstract
Nanomaterials are those materials that have at least one dimension at nanoscale (less than 100nm). In this current study, the magnetic, electrical, spectral properties of nanomaterials were studied. Magnetic Properties of Nanoparticles refers to magnetic materials such as super-paramagnetic materials and magnetic susceptibility, related phenomena in super-paramagnetic particles, application of superparamagmetic materials, exchange-coupled magnetic nanomaterial specimens are classified in response to an external magnetic field. Electrical Properties of Nanoparticles discuss about the basis of electrical conductivity in nanotubes and nanorods, carbon nanotubes, photoconductivity of nanorods, electrical conductivity of nanocomposites. Characterization of Nanomaterials includes aspects on global methods for characterization, specific surface are X-Ray and electron diffraction, electron microscopy and in general consideration, with the interaction of the electron beam and specimen, localized chemical analysis in the electron microscope, scanning transmission electron microscopy uses a high-angle annular dark-field (HAADF) detector. With the help of magic angle spinning, solid state Si^{29} and Al^{27} NMR spectroscopy was used to detect two types of smectites, types of illites and a type of vermiculite. In the current research, naturally occurring samples were used. These were arranged in a ratio 2:1 clay mineral. Al^{27} NMR spectroscopy was used to describe the coordination of aluminum with the tetrahedron. Si^{29} NMR spectroscopy was used to observe the coordination of aluminum with other compound and also to detect chemical nature of interlayer species.

Keywords: interlayer, spinning, vermiculite, tetrahedron

1. Introduction

Nanomaterials

Nanomaterials are those materials where the size of the individual building block is less than 100 nm, at least in one dimension. The second definition is much more restrictive, and states that nanomaterials have properties which depend inherently on the small grain size and, as nanomaterials are usually quite expressive, such a restrictive definition makes more sense. These are free surface in the case of particulate materials, or grain boundaries in bulk material.

Nanomaterials have large surfaces, which can be demonstrated by using spherical particles as examples. Phase transformations are connected with a change in physical properties, and it is the density of the material that is diverted in most cases. Phase transformation may be caused by the temperature change that occurs due to the coagulation of two particles. The process of particle formation may be divided into two major steps: nucleation, condensation of atoms.

Auger electron spectroscopy (AES) and X-ray photonelectron spectroscopy (XPS) can be utilized to characterize the surface impurities to a depth of 0.5-1 nm with a spatial resolution of 0.2 μm for AES and 0.2 mm for XPS, and a sensitivity of 0.3%.

Techniques Used for the Formation of Nanoparicles

Sol-gel Technique

The sol–gel technique has been implemented to prepare silver nanoparticles and silica nanospheres [16]. This method involves the hydrolysis of salts. Ultrapure or homogeneous multi-component glasses can be made by sintering at a temperature well below the liquid temperature of the system. The process usually begins from alkoxide compounds through hydrolysis and poly-condensation at room temperature. One particular example is the reaction of tetraethylthio-silicate (TEOS), Si $(OC_2H_5)_4$, ethanol and water. These three reactants form one phase solution after stirring molecules, coagulation by exchange of surface energy. The process is explained in Eq 1 and 2.

$$Si(OC_2H_5)_4 + 4H_2O \rightarrow Si(OH)_4 + 4C_2H_5OH \ldots\ldots\ldots \text{Eq.1}$$
$$Si(OH)_4 \rightarrow SiO_2 + 2H_2O \ldots\ldots\ldots\ldots\ldots\ldots\ldots \text{Eq.2}$$

Inert Gas Condensation

The most important and certainly the oldest process for synthesizing nanoparticles in the gas phase is that of inert gas condensation. This process is applied to thermal evaporation to a metal particle within a vacuum chamber filled with a small amount of inert gas. The basic principle may lead to many variations, such as the systems employed are different in the metal introduced and subsequently evaporated.

When used as a heat source for mass production, an electrical arc is used which have many advantages and is utilized on a regular basis by transport via thermal diffusion using a carrier gas. When use as a heat source for mass production, an electrical reservior has been used. One of the most interesting possibility is heating with an electron beam. The technical scale-up of an inert gas condensation process may lead to the introduction of the elements that limits particle size growth.

However, two possible measures may exist through which particle size and particle size distribution may be controlled: (i) a decrease in the existing time of the particles in the reaction zone; and (ii) rapid cooling of the particles which have left the reaction zone thereafter. Both can measure the

original diffusion-controlled mechanism. It is necessary to transport via a thermal diffusion using a carrier gas.

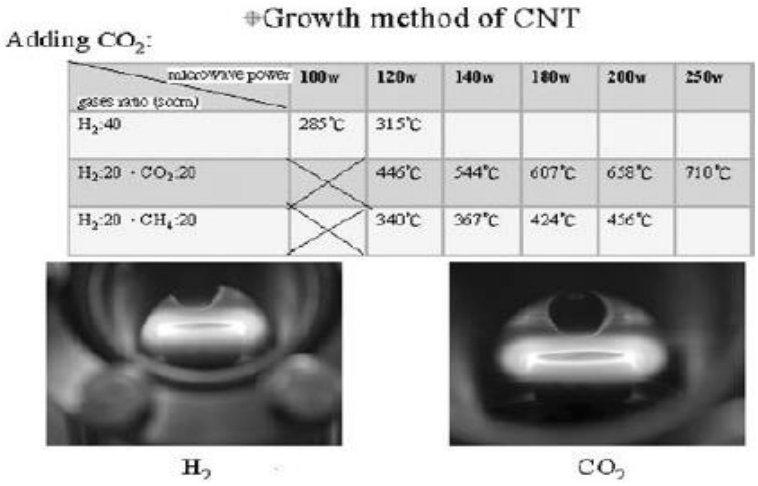

Fig 1: The colors of the plasma balls for flow gases to be hydrogen and carbon dioxide are shown on the left and right columns in Figure 4(a), respectively, where the flow of carbon dioxide can sharply increase the plasma temperature to white color. Reprinted with permission from [56], S. Y. Chen et al., *J. Nanosci Nanotechnol.* 5, 1987 (2005). © 2005, American Scientific Publishers.

Properties of Nanoparticles

Physical Properties

Carbon nanotube becomes one of the most promising materials in recently developed materials on account of its superior properties of rigidity, strength, elasticity, electric conductivity, and field emission.

The conductivity of the electrodes before CNT growth is almost negligible small inferring the insulation of the SiO_2 layer. The gap width is 3nm and the CNT wire diameter is about 100 nm from an inspection of a SEM. The structure of the carbon nanofibre is not straight as expected. The ideal ohmic contact is verified by measuring the contact resistance after growth. Figure 5 dictates the current–voltage (I–V) characteristics at various temperatures with each data to be the averaged of twenty repetitive measurements. The curves illustrate a step at temperatures below 100 K occurring at a rather high current density implicitly inferring that this phenomenon is difficult to be observed if the CNT is not so rigidly grown from the catalyst electrodes. The straight line within this current range reveals the ohmic contact whilst the nonlinear properties at even higher currents might be due to the space charge limits. Current at the step conductance decreases as the measuring temperature becomes lower and the step becomes prominent. At 20 K the step occurs at the bias of ±150 mV that is justified by the carrier jump from one quantum level to another exhibiting a discontinuous of transport at this voltage. The logarithm of the normalized conductance at the specified voltage log G/G_0 expressing a sharp dip at ±150 mV, where G is the conductance

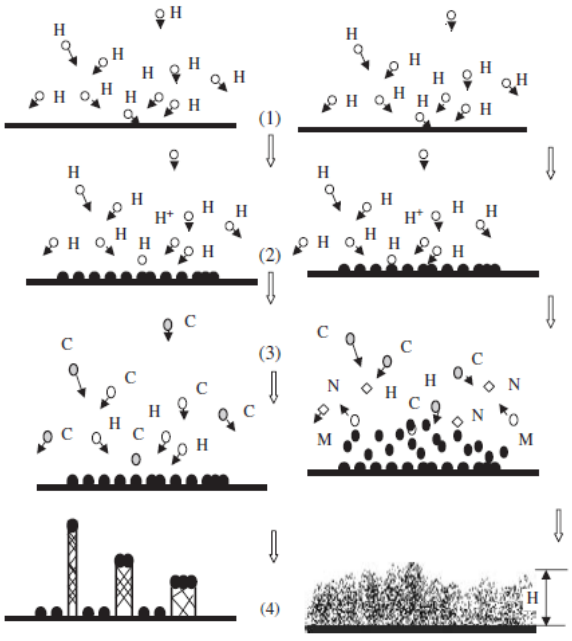

Fig 2: Pictorial mechanisms for CNT growth for dilute gas in (right column) pure hydrogen, (left column) hydrogen and ammonia. Substrates are etched at steps from up to down to produce nanostructured surface. Reprinted with permission from [50], A. Gorbunov et al., *Appl. Surf. Sci.* 197–198, 563 (2002). © 2002, Elsevier.

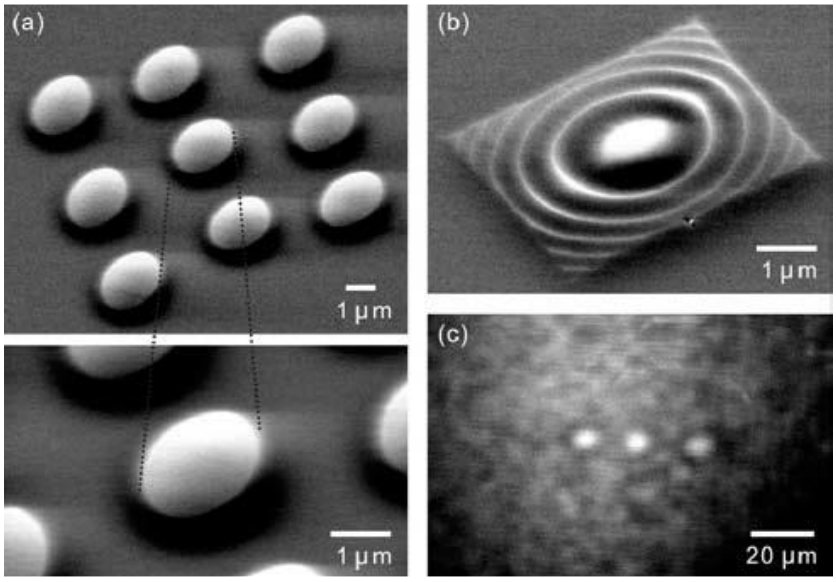

Fig 3: (a) Scanning electron micrograph. Using an atomic-force microscope (AFM) gray scale patterning technique, microlenses arrays can be fabricated with superior focal length capability and low surface roughness values of approximately 1 nm. (b) Scanning electron micrograph. The process also allows for fabrication of unusual or arbitrarily shaped microlenses, and is difficult if not impossible to create using standard resist reflow techniques. (c) Infrared optical image of one 1×3 microlens array, confirming the focusing function of AFM-patterned Si microlenses.

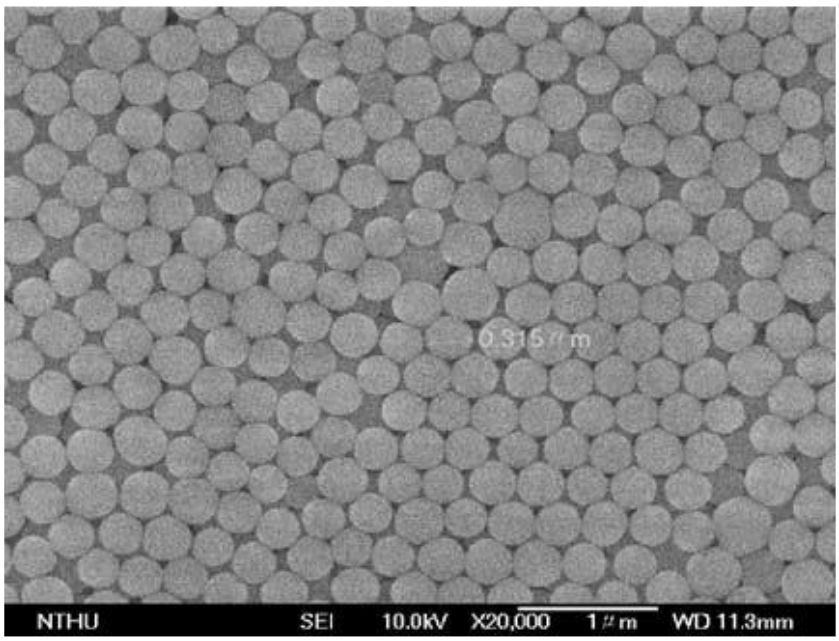

Fig 4: The SEM photographs of silica plates prepared at PH = 9-2 after 4 days.

Magnetic Properties

Magnetic Properties of Nanoparticles refers to magnetic materials such as super-paramagnetic materials and magnetic susceptibility, related phenomena in super-paramagnetic particles, application of superparamagmetic materials, exchange-coupled magnetic nanomaterials. Materials are classified in response to an external magnetic field. Classification of materials represents diamagnetic, paramagnetic and ferromagnetic. Although, all materials shows inherited diamagnetic properties, only those materials which are not paramagnetic or ferromagnetic in nature does not show diamagnetic properties. Super paramagnetism is a property of isolated non interacting particles. The majority of successful applications of magnetic nanomaterials use particulate composites with super paramagnetism being necessary for the application of two main reasons:

- Super paramagnetic particles avoid magnetic clustering;
- Super paramagnetic particles may be either attracted or released by switching the magnetic field.

From an economic point of view, the most interesting applications of super paramagnetic nanoparticles are related to medicine and biology.

Electrical Properties

Electrical Properties of Nanoparticles discuss about the basis of electrical conductivity in nanotubes and nanorods, carbon nanotubes, photoconductivity of nanorods, electrical conductivity of nanocomposites. In electrically conducting carbon nanotubes, only one electron wave mode is observed which transport the electrical current. As the lengths and orientations of the carbon nanotubes are different, they

touch the surface of the substrate at different time, which provides information about the influence of carbon nanotube length on the resistance. Then with increasing extension of the fiber bundle, an increasing number of carbon nanotubes will touch the surface of the substrate and contribute to the electrical current transport.

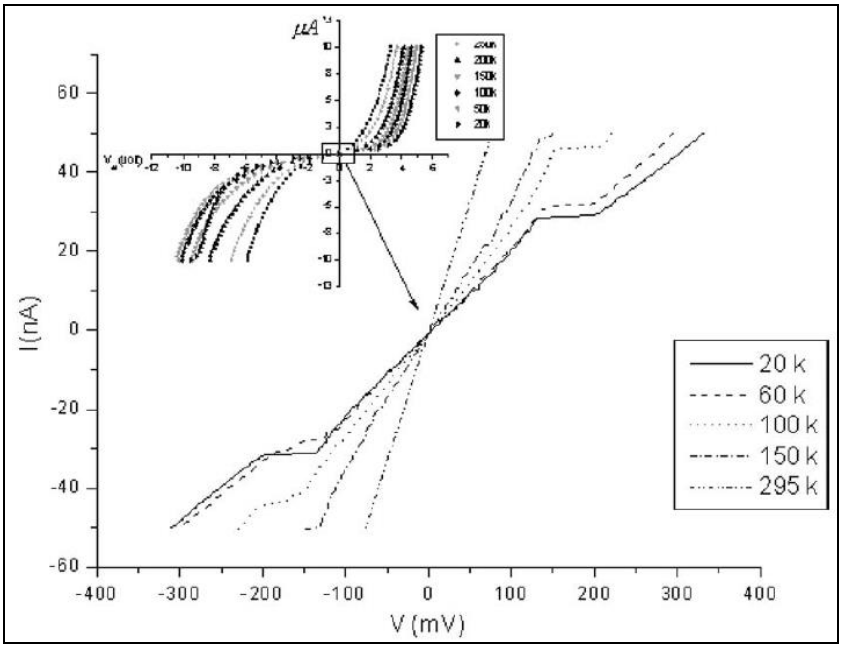

Fig 5: The I–V characteristic of one carbon nanofiber. Reprinted with permission from [119], L. W. Chang and J. T. Lue, *J. Nanosci. Nanotechnol.* 5, 1672 (2005). © 2005, American scientific Publishers.

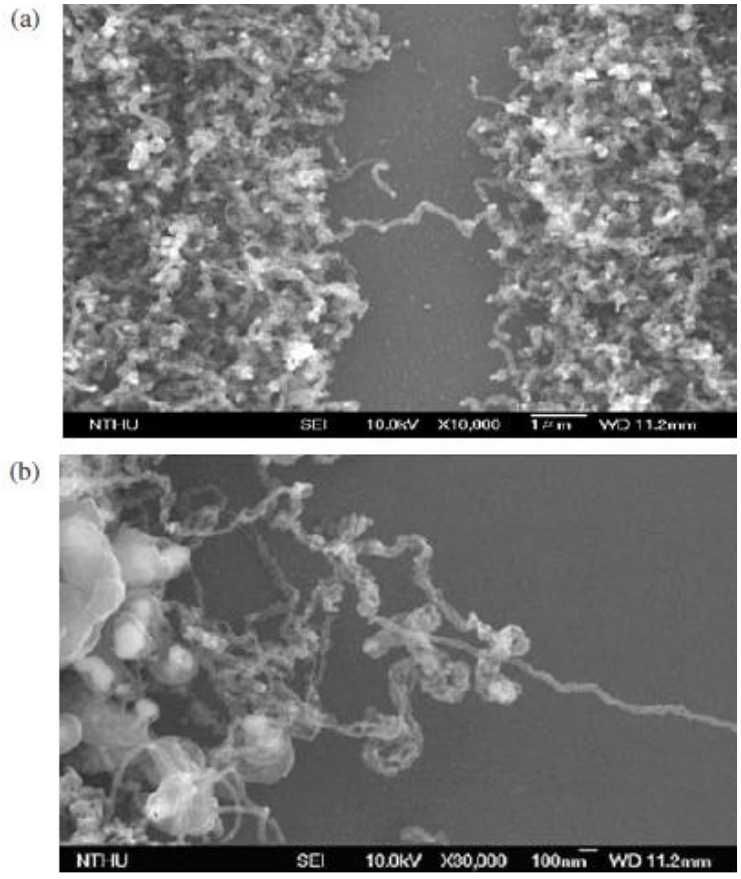

Fig 6: (a) A single carbon nanofiber grown across isolated electrodes as a current conduction bridge, (b) the root of the single fiber is multi-connected to nickel electrodes. Reprinted with permission from [56], S. Y. Chen et al., *J. Nanosci. Nanotechnol.* 5, 1987 (2005). © 2005, American Scientific Publishers.

Characterization of Nanomaterials

Characterization of Nanomaterials includes aspects on global methods for characterization, specific surface area, X-Ray and electron diffraction, electron microscopy and in general consideration, with the interaction of the electron beam and specimen, localized chemical analysis in the

electron microscope, scanning transmission electron microscopy uses a high-angle annular dark-field (HAADF) detector. The most important among the latter group of methods are those that are microscopic in nature. The behavior of nanomaterials is controlled by their global properties, which provides indications by which an assembly behaves.

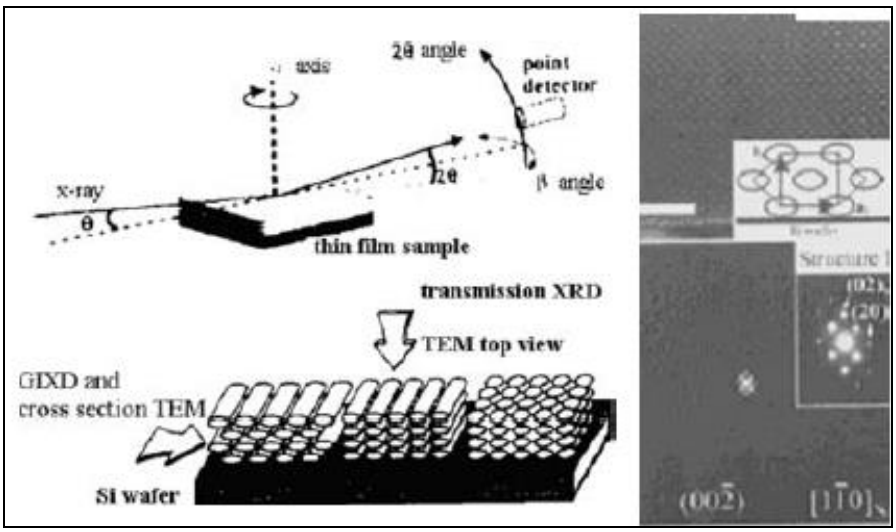

Fig 7: Schematic illustration of the XRD experiments, the three dimensional pore structure in SiO_2 film, and the TEM image Reprinted with permission from [68], P. T. Liu et al., *J. Appl. Cryst.* 38, 211 (2005). © 2005

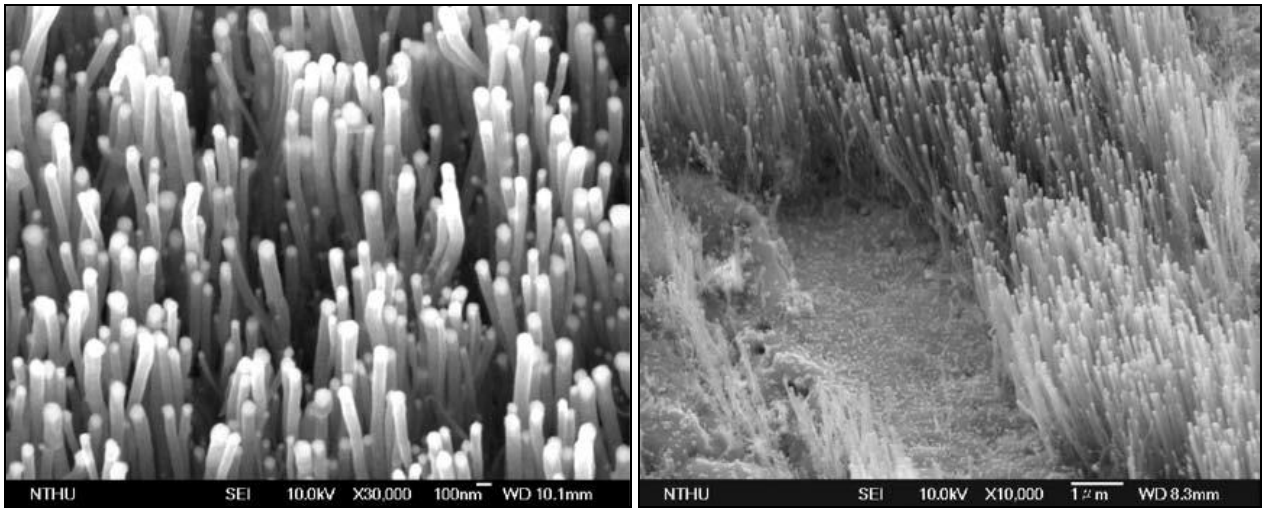

Fig 8: SEM of (a) well aligned and flourished growth of CNTs on a Cu-10 wt% Fe-10 wt% Co-10 wt% Ni bulk alloy substrate, and (b) exaggeration of the right part of (a) showing upright tubes embed with catalyst particle at tips. Reprinted with permission from [53], S. Y. Chen et al., *J. Phys. D.: Appl. Phys.* 37, 273 (2003). © 2003, Institute of Physics.

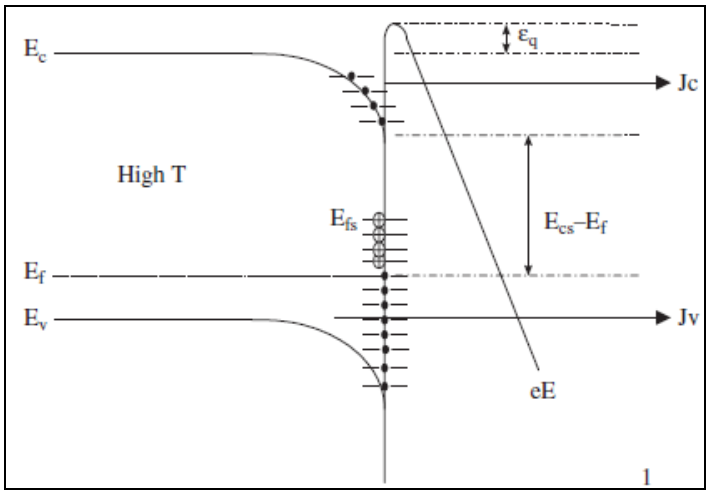

Fig 9: Schematic energy band diagrams for (a) high temperature; and (b) low temperature, respectively. Reprinted with permission from [98], S. Y. Chen et al., J. Phys. D: Appl. Phys. 37, 273 (2004). © 2004, Institute of Physics.

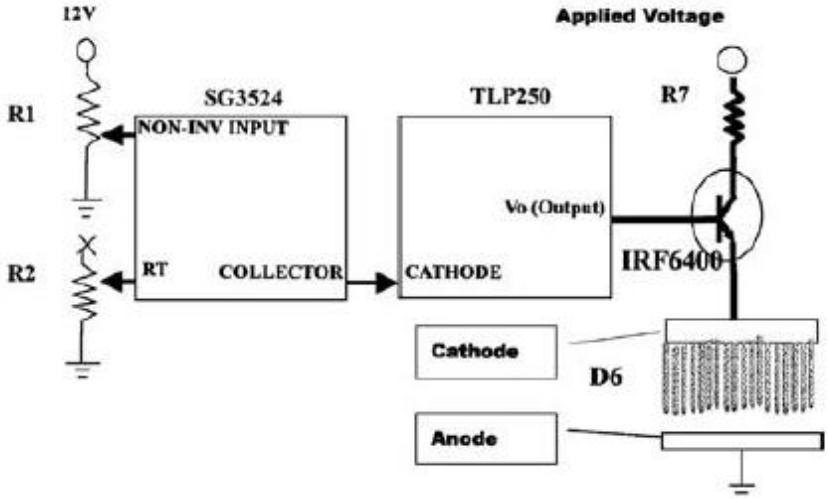

Fig 10: The schematic diagram of the electronic circuit to perform the micro-EDM process that generates the desired on and off cycles

With the help of magic angle spinning, solid state Si^{29} and Al^{27} NMR spectroscopy was used to detect two types of smectites, types of illites and a type of vermiculite. These were arranged in a ratio 2:1 clay mineral. Al^{27} NMR spectroscopy was used to describe the coordination of aluminum with the tetrahedron. Si^{29} NMR spectroscopy was used to observe the coordination of aluminum with other compound and also to detect chemical nature of interlayer species. In the current research, naturally occurring samples were used. These samples were mixed in the ratio of 2:1. The samples were treated with 1M solutions of alkali, alkaline earth metal, lanthanide and amine HCL salts at a temperature of 40-50 ^{0}C for specific time period. Si^{29} NMR and Al^{27} NMR spectra were observed at a value of 59-61MHz and 78-19 MHz respectively on Bruker CXP-300 NMR spectrophotometer at Brisbane NMR center, Griffith University. Samples were utilized in delrin rotors and usually it was spun at 3-4 kHz. Well resolved resonances in vermiculite at δ= -84.6, -88.7 and -92.9ppm were assigned to Q^3(2Al), Q^3(1Al), Q^3(0Al) respectively. The bentonite clay and montmorillonite clay showed one resonance center at δ= -93 Q^3(0Al). The illites showed wide range of resonance between δ= -80 and δ= -105. The spectrum of Si^{29} complexed with alkyl ammonium cations displayed a shielding in a range of 1ppm in contrast to untreated samples. Additionally, IR studies (Farmer and Russell, 1967) [4] have discovered that a mechanism of hydrogen bonding proceeds because of structural oxygen and interlayer species like water. This has been further confirmed by proton NMR. Regardless of the identity of the interlayer cations or the degree of hydration, a given hydrated smectite or vermiculite would be expected to display a similar spectrum of Si^{29}. Small cations were involved in influencing the study of silicates.

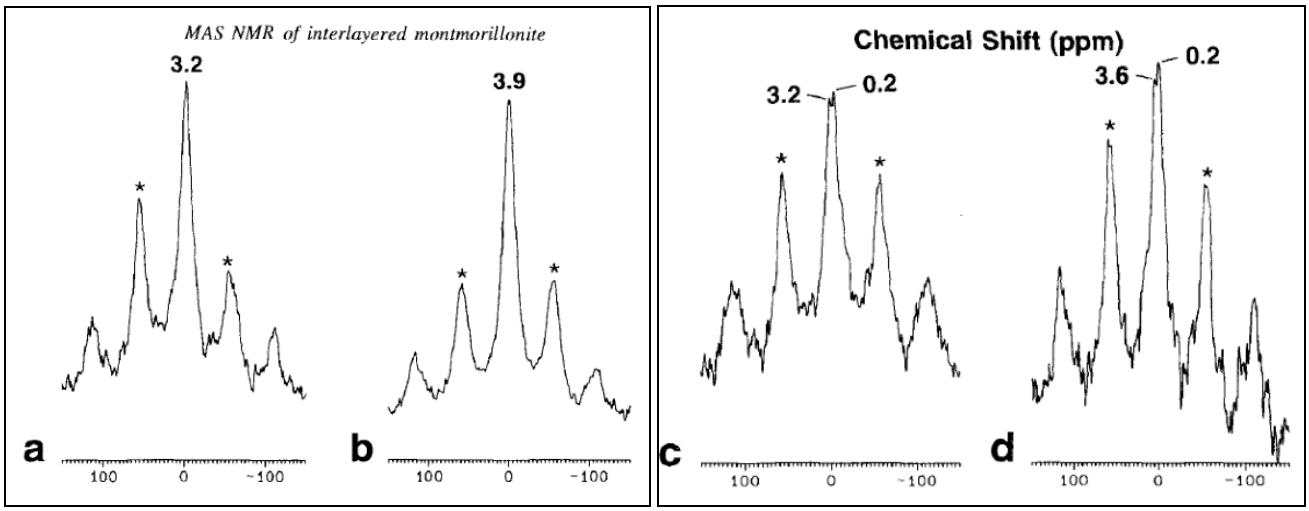

Fig 11: 27AI MAS NMR spectra of (a) the control; (b) Al-clay; (c) two coprecipitated clays where the Al/(Al+Cr) molar ratio = 0.5; and (d) = 0.33. Asterisks indicate SSBs

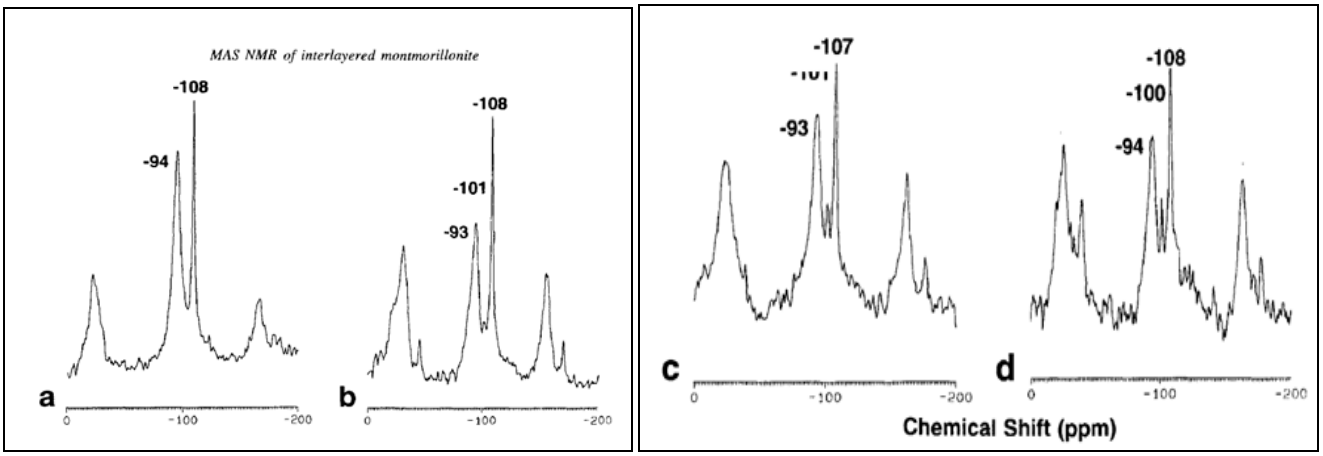

Fig 12: 29Si MAS NMR spectra of **(a)** the control; **(b)** coprecipitated clay where the Al/(Al+Cr) molar ratio = 0.33: **(c)** of two Cr-clays where the amount of sorbed Cr (cmol Cr3Vkg) is 200; and **(d)** 355. Asterisks indicate SSBs

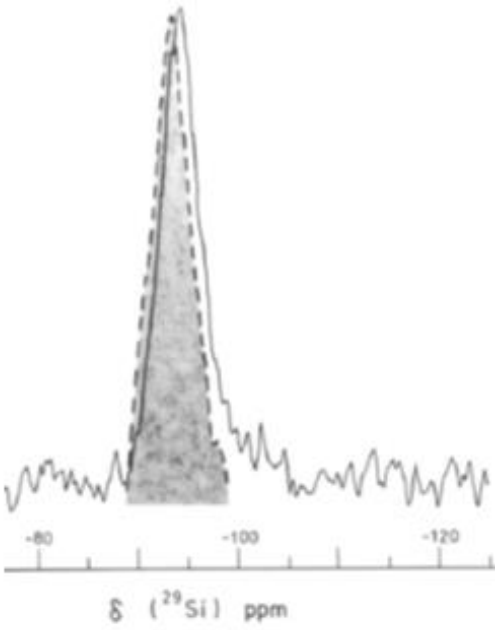

Fig 13: Si DD/MAS spectrum of Polkville montmorillonite treated with I M ethylene liammonium chloride solution at 40°C for I week. The overlain signal (shaded) is that of the corresponding Ca-montmorillonitc

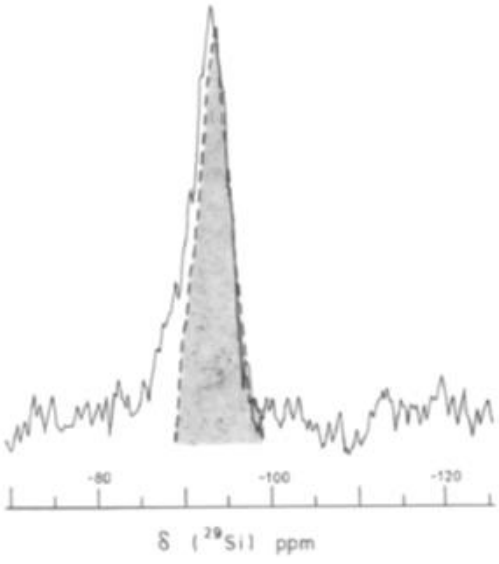

Fig 14: 29Si DD/MAS spectrum of Polkville montmorillonite treated with 1 M anilinium chloride olution at 40°C for I week. The overlain signal (shaded) is that of the corresponding Ca-montmorillonite

4. References

1. Alagarasi A. Introduction to Nanomaterials (Chapter 1), 2011, 76.
2. Gorbunov A, *et al*. Appl. Surf. Sci. Elsevier. 2002; 563:197-198.
3. Book review Environmental Engineering and Management Journal **7.** 2008; 6:865-870.
4. Farmer VC, Russel JD. Infrared absorption spectrometry in clay studies. Clay's Clay mineral. 1967; 15:121-124.
5. Chang LW, Lue JT, J Nanosci. Nanotechnol. (2005). American scientific Publishers. 2005; 5:1672.
6. Klein LC. Sol-Gel Technology for Thin Films, fibers, Preforms, Electronics, and Specialty Shapes. Noyes Publications, 1988; CJ Brinker and G. W. Scherer, Sol–Gel Science. Academic Press, San Diego, 1990.
7. Lochhead MJ, Bray KL. Chem. Mater. 1995; 7:572.
8. Liu PT, *et al*. J Appl. Cryst. 2005; 38:211.
9. Chen SY, *et al*. J Nanosci Nanotechnol. American Scientific Publishers. 2005; 5:1987.
10. Chen SY, et al. J. Phys. D.: Appl. Phys. 2003; 37:273. © 2003, Institute of Physics.
11. Chen SY, et al. J. Phys. D: Appl. Phys. 2004; 37:273. ©, Institute of Physics.